Determination of spatial charge separation of diffusing electrons by transient photovoltage measurements

Iván Mora-Seró[a)]
Departament de Ciències Experimentals, Universitat Jaume I, E-12080 Castelló, Spain

Thomas Dittrich
Hahn-Meitner-Institute, Glienicker Strasse 100, 14109 Berlin, Germany

Germà Garcia-Belmonte and Juan Bisquert
Departament de Ciències Experimentals, Universitat Jaume I, E-12080 Castelló, Spain

(Received 4 May 2006; accepted 7 August 2006; published online 22 November 2006)

It is shown that the surface photovoltage produced by the photoinjected carriers in a layer can be split up into two contributions: total amount of charge, and distance between the centers of charge of the positive and negative carriers. This fact allows us to extract information directly about spatial charge separation of photoinduced charge and its time evolution from surface photovoltage transients. Two cases of particular experimental relevance are analyzed in detail to show the generality of the method: Diffusion photovoltage and tunneling recombination in layers with thickness less than the screening length, and in layers thicker than the screening length, considering also the limit case of diffusion in a semi-infinite space. © *2006 American Institute of Physics*. [DOI: 10.1063/1.2361158]

I. INTRODUCTION

The surface photovoltage (SPV) method is a well-established material characterization technique which relies on analyzing the illumination-induced charges in the surface photovoltage.[1] SPV is a contactless method, which makes it extremely attractive for the characterization of a wide spectrum of materials, including inorganic semiconductors and dielectrics,[2] porous semiconductors,[3] and organic semiconductors.[4,5] One of the multiple variants of this technique studies the time evolution of SPV after the sample was illuminated with a laser pulse. This specific method allows investigation of the carrier diffusion and recombination processes in the sample.[1–3,6–8]

The surface photovoltage (SPV) method is locally sensitive with respect to a charge separation length, in contrast to other photoelectrical techniques that provide macroscopic and time-averaged parameters, such as photocurrent measurements. Charge separation plays a crucial role in many biological, chemical, and physical systems, and time-resolved SPV can be used to study the charge separation process in very short distances of the order of nanometers. Regarding a parallel plate capacitor, a separation of only 1 nm of positive and negative charges with a density of 10^{12} cm^{-2} will already lead to a potential difference of the order of 5 mV, which can be nicely measured by transient methods. This makes the SPV method interesting for charge separation studies even on molecular systems which do not have a space-charge region. In order to facilitate the physical interpretation, it seems quite interesting to develop a formulation capable of directly relating the SPV signal with the spatial charge separation.

Young investigated the kinetics of xerographic discharge by surface charge injection employing a simple method based on the surface potential.[9] He derived several expressions relating the surface potential with the spatial distribution of carriers. Following an analogous procedure, we show in this paper that the SPV, normally expressed as the double integration of the Poisson equation, can also be obtained directly from the extent of charge separation.

In the case of xerographic process high voltage and carrier densities are usually obtained, producing space-charge limitation, and consequently the diffusion current of the carriers is neglected in favor of the drift current that rules the transport process. In this case the study of the surface potential decay in insulators is a useful method to determine the drift mobility.[10] We extend this study considering that the transport of the carriers is governed mainly by diffusion instead of drift of the electrical field. This assumption applies for the low carrier density and surface potential induced by light, and the small size (~nm) of the samples. Indeed Wright studied the mechanism of space-charge-limited current in solids,[11] showing that the drift mechanism becomes predominant for high voltage, as in the case of the corona discharge of the xerography, and at large distances. However, in the thin region near the injection cathode, the transport is governed by diffusion, and by drift in the remaining volume of the sample. Additionally, the drift contribution to transport has been evaluated in the cases that we show in this paper; it has been observed that it is negligible with respect to diffusion contributions.

The picture of the parallel plate capacitor can be transferred to photoinduced charge separation, introducing a charge separation length as the difference between the centers of positive and negative excess charge. For conventional semiconductors, this is trivial since the charge separation length is given by the extension of the fixed space-charge

[a)]Author to whom correspondence should be addressed; electronic mail: sero@exp.uji.es

region. However, the situation can be completely different, for example, in systems with very low densities of equilibrium charge carriers or very low diffusion coefficients. In such systems, the charge separation length may change in time by independent diffusion of excess electrons and holes.

Here, we analyze theoretically the interpretation of the SPV transients for investigating the charge separation process. Specifically we show that the time evolution of SPV generated by the photoinduced charges can be split up into the product of the total amount of charge times the charge separation length, as a consequence of the superposition principle. This result allows information about spatial charge separation from transient photovoltage measurements to be gained directly, making this technique extremely attractive for the study of charge separation in a wide range of materials.

In the next section we formulate the problem of interpretation of SPV in more concrete terms. To exemplify the study of SPV under this new point of view we will consider the cases of diffusion photovoltage induced by the photoinjection of carriers in layers with thickness less than the screening length and in layers thicker than the screening length, considering also the limit case of diffusion in a semi-infinite space. The main conclusions of the work will be presented in the final section.

II. SURFACE PHOTOVOLTAGE AND CENTER OF CHARGE

Let us consider a simple model system, consisting of a layer with a sheet of positive charge at the outer surface, $x=0$, as schematized in Fig. 1(a), and a distribution of electrons $n(x,t)$, in cm^{-3} units, diffusing into the layer with a thickness L_S, as indicated in Fig. 1(b). Such a system can be realized, for example, by injection of electrons from neutral molecules adsorbed at the surface[7,8]. The total number of electrons per unit area at time t,

$$N(t) = \int_0^{L_S} n(x,t)dx, \tag{1}$$

is the same as the number of fixed positive charges. The measured SPV corresponds to the voltage $U(t)$ created by the separation of charge. The electrical field $E=-\partial U/\partial x$ across the distribution is related to the electron density by Poisson's equation

$$\frac{\partial E}{\partial x} = -\frac{ne}{\varepsilon\varepsilon_0}, \tag{2}$$

where e is the elementary charge, $\varepsilon_0=8.85\times10^{-14}$ F/cm, and ε is the dielectric constant of the layer. With a first integral of Eq. (2) we obtain (Gauss law)

$$E(x,t) - E(0,t) = -\frac{e}{\varepsilon\varepsilon_0}\int_0^x n(y,t)dy. \tag{3}$$

We can assume that the electrical field at a certain point $x=L_S$ is zero. Reasons for this may be screening[8] or considering the layer as semi-infinite. From a second integration of the Poisson equation, the SPV transient is given by

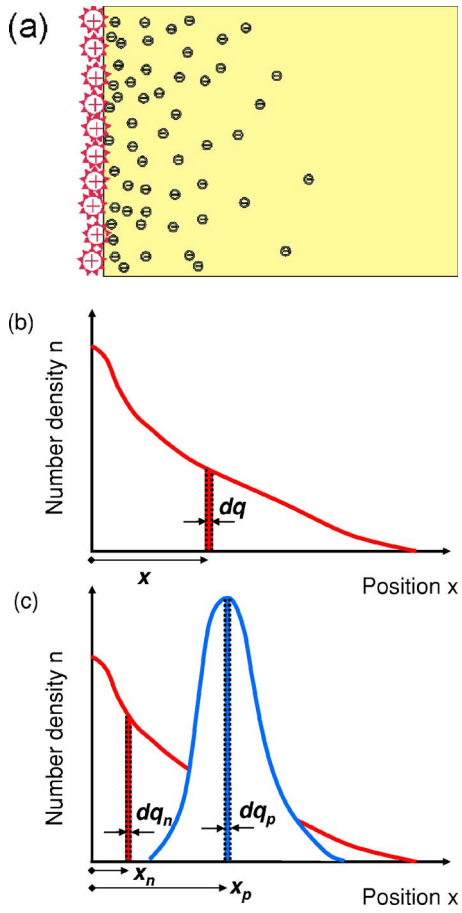

FIG. 1. (a) Schematic representation of electrons injected from dye molecules into a material layer. (b) Spatial distribution of electrons considering that the same total amount of positive charges is fixed at $x=0$; a thin slice of $dq=e\,n\,A\,dx$ at x position is indicated. (c) Spatial distribution of positive and negative charge considering that the total amount of both is equal; a thin slice of negative, dq_n, and positive charge, dq_p,at a distances x_n and x_p, respectively, is indicated.

$$\mathrm{SPV} = U(t) = \frac{e}{\varepsilon\varepsilon_0}\int_0^{L_S} dx\int_0^x n(y,t)dy. \tag{4}$$

In most previous work, the SPV has been calculated using Eq. (4).[12] Now, we aim to obtain an expression that relates $U(t)$ to a first spatial integral of the charge density.

Before an analytical derivation of the SPV expression as the product of the total amount of charge and the charge separation length, we show a simple model, based on the plane capacitor picture, which allows an easy interpretation and visualization of the problem. An alternative way to Eq. (4) for the calculation of the photovoltage induced by the electronic distribution is to take the summation of the voltage produced for each thin slice of differential charge dq, considering a plane capacitor with the same amount of charge dq, but with an opposite sign, situated in the surface at $x=0$, and with a separation x between plates; see Fig. 1(b). Each slice produces a differential voltage,

$$dU(t) = \frac{dq}{C} = \frac{x\,dq}{\varepsilon\varepsilon_0 A}, \tag{5}$$

where C is the capacity and A is the area. Taking into account the distribution of electrons,

$$e\, n(x,t) = \frac{dq}{A\, dx} \tag{6}$$

the total SPV can be calculated, considering the superposition principle, integrating Eq. (5):

$$\mathrm{SPV}(t) = \frac{e}{\varepsilon\varepsilon_0} N(t)\langle x\rangle(t), \tag{7}$$

where $\langle x\rangle(t)$ is the mean position of the electrons, i.e., their center of charge,

$$\langle x\rangle(t) = \frac{1}{N(t)} \int_0^{L_s} x\, n(x,t) dx. \tag{8}$$

This model, with a sheet of positive charge fixed at the outer edge, $x=0$, can be easily extended to a more general model that takes into account spatial distributions of both positive and negative carriers in the bulk [see Fig. 1(c)], with the same total amount of charge of each carrier, which is the case in SPV measurements.

Now, let us consider that there are total amounts of positive and negative charge fixed at $x=0$, which are equal to the total amount of negative and positive charge in the bulk of the sample. This is allowed mathematically since the total amount of charge at $x=0$ is zero. The negative charge distribution will contribute to SPV by the same quantity as in Eq. (7). We can obtain the contribution of the positive charge distribution in the same way but with opposite sign, obtaining finally

$$\mathrm{SPV}(t) = \frac{e}{\varepsilon\varepsilon_0} N(t)(\langle x_n\rangle(t) - \langle x_p\rangle(t)), \tag{9}$$

where $\langle x_n\rangle(t)$ is the center of negative charge as defined in Eq. (8), and $\langle x_p\rangle(t)$ is the center of positive charge as defined in Eq. (8) with $p(x,t)$ instead of $n(x,t)$. We consider the charge separation length as $\langle x_n\rangle(t) - \langle x_p\rangle(t)$. The value of $N(t)$ is the same for both distributions because recombination reduces identically positive and negative charge. Equation (9) illustrates that the SPV signal is proportional both to surviving charge and charge separation length.

For an analytical derivation we consider again that the positive charge is fixed at $x=0$. The Poisson equation (4) for the SPV can be expressed as

$$\mathrm{SPV}(t) = \int_0^{L_S} E(x,t) dx. \tag{10}$$

Integrating by parts,

$$\mathrm{SPV}(t) = xE(x,t)_0^{L_S} - \int_0^{L_S} x \frac{\partial E(x,t)}{\partial x} dx, \tag{11}$$

which is the same expression obtained by Young.[9] In our case, as it has been pointed out, $E(L_S,t)=0$, and introducing Eq. (2) in Eq. (11), we arrive at the same result for the SPV as the one expressed in Eq. (7). As before, this result can be easily extended to the general case where the positive charge distribution is not localized at $x=0$, obtaining Eq. (9). It is important to remark that this result is valid for any space-charge distribution and for any possible time evolution, if the amount of positive and negative charge remains equal, independently of the processes that originated this time evolution. This will allow us to predict and to understand readily SPV transients, as we show in the next two sections as examples.

III. DIFFUSION PHOTOVOLTAGE IN LAYERS WITH THICKNESS LESS THAN THE SCREENING LENGTH

In this section, in order to show the generality of the proposed method, we discuss the spatial charge separation process in an ultrathin layer, i.e., one in which the moving carriers reach the blocking boundary opposite the injection surface. We consider that the layer thickness is less than the screening length, i.e., all the charge diffusing in the sample contributes to the photovoltage. We also consider the important effect of the recombination of injected carriers with the parent molecules in the charge transport. Recently, we have shown that the photovoltage transients produced by the diffusion of dye-photoinjected electrons in ultrathin TiO_2 layers, with thickness d can be explained qualitatively considering a tunneling recombination coupled with a diffusion process.[7] The distribution of the photoinjected electrons can be obtained integrating the continuity equation,

$$\frac{\partial \Delta n(x,t)}{\partial t} = D \frac{\partial^2 \Delta n(x,t)}{\partial x^2} - \frac{\Delta n(x,t)}{\tau_0} e^{-2x/a}, \tag{12}$$

where τ_0 is a phenomenological parameter, the lifetime for vanishingly small spatial separation, and a is the electrons Bohr radius. Equation (12) has been solved numerically by the method of finite differences considering blocking boundary conditions at both the dye/TiO_2 and TiO_2/substrate interfaces $[(\partial n/\partial x)_{x=0,\, L_S}=0]$. The SPV signal dependence on the electron distribution can be found by integrating the Poisson equation, Eq. (4). We will show that Eq. (7) also gives an accurate description of the SPV transients within the errors induced by the numerical calculations.

We assume that the distribution of photoinjected electrons at the initial time, $t=0$, is exponential with a preexponential factor n_0, and with the width controlled by a b parameter.[7,13] Figure 2 shows the results of the numerical integration of Eqs. (4), (7), and (12) for four different diffusion coefficients. Figure 2(a) plots the time evolution of $N(t)$, which displays nearly constant values for $t < \tau_0$ and a decay for $t > \tau_0$ due to the effect of recombination. In Fig. 2(b) the time evolution of $\langle x\rangle(t)$ is represented. For cases with nonzero diffusion coefficient there is a progressive increase of $\langle x\rangle(t)$ with time due to charge separation by diffusion, until for certain t_s, $\langle x\rangle(t)$ reaches a constant value $\langle x\rangle_{ct}$. This leveling of the charge separation is originated by the finite nature of the sample. When the center of charge is used to calculate the surface photovoltage, Fig. 2(c), it is determined by the product of the magnitudes plotted in Figs. 2(a) and 2(b), as indicated by Eq. (7). As expected, the photovoltage calculated using the Poisson equation and using the center of charge present close values, especially for longer times because the time step used in the numerical integration was the same in all the time range, inducing higher errors at low

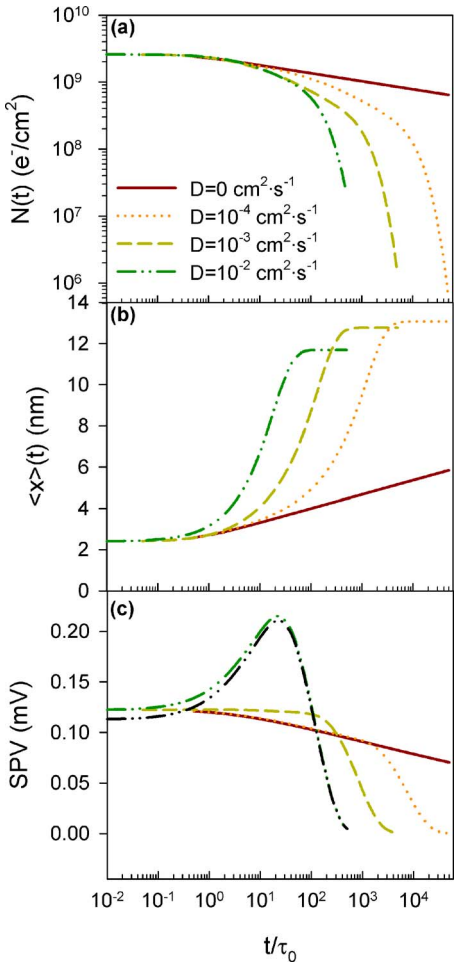

FIG. 2. Patterns of (a) $N(t)$, (b) $\langle x\rangle(t)$, and (c) SPV obtained from the Poisson equation, obtained from numerical simulation for different diffusion coefficient, D; the simulation parameters employed are $L_s=20$ nm, $n_0=10^{16}$ cm^{-3}, $\tau_0=2$ ps, $a=0.6$ nm, and $b=2.5$ nm. In (c) it is also plotted in black the SPV obtained from the $\langle x\rangle(t)$ value employing Eq. (7), with $D=10^{-4}$ cm^2 s^{-1}, for comparison.

times. These results indicate that the analysis of the SPV allows study of the spatial charge separation.

In the case without diffusion there is no significant feature in the SPV pattern. $\langle x\rangle(t)$ increases with time due to the fact that the tunneling is spatially dependent and stronger close to the dye at $x=0$. But, this increase is not enough to compensate for the reduction of the SPV due to the diminution of charge. When a nonzero but low diffusion coefficient is employed in the simulations, $D=10^{-4}$ cm s^{-1}, the diffusion produces an increase of the charge separation, Fig. 2(b), not enough in this case to overcome the effect of the charge reduction by recombination, and only a slight increase of the photovoltage is observed at low times in comparison with the SPV obtained for zero diffusion coefficient. Nevertheless, a characteristic feature is noted in this decay, a shoulder after which a decrease is observed at t_{shoulder}, faster than in the case of $D=0$. This feature is originated by the back diffusion of the electrons. At the initial time the large gradient originated by the exponential distribution induced by the injection produces the diffusion of the injected electrons toward the back contact, increasing $\langle x\rangle(t)$, as shown in Fig. 2(b). The diffusion tends to transform the initial exponential charge distribution into a flat distribution without density gradients, but the high reduction of electrons near $x=0$ produces a reverse density gradient for high times, indicating that $\langle x\rangle_{ct}$ saturates for values higher than $d/2$. This reverse gradient also produces back diffusion of the electrons to the region with high recombination probability, originating the fast decay in the SPV observed in Fig. 2(c), in which the recombination is assisted by the diffusion.

When a higher diffusion coefficient is employed in the simulations, $D=10^{-3}$ cm^2 s^{-1}, the diffusion produces an important increase of the charge separation that partially compensates the effect of the charge reduction by recombination at low times, obtaining a higher SPV value for low times, Fig. 2(c); but, this higher diffusion coefficient also enhances the back diffusion and consequently t_{shoulder} and the fast SPV decay are obtained at lower times than for the previously analyzed diffusion coefficients. For the case of the highest diffusion coefficient employed, $D=10^{-2}$ cm^2 s^{-1}, the rapid charge separation is much faster than the recombination. The increased extent of charge separation overcomes the effect of reduction of charge and produces the apparition of a SPV peak at t_{peak}.

Comparing the time in which $\langle x\rangle_{ct}$ attained, Fig. 2(b), with the time in which the characteristic feature, shoulder or peak, is observed in the SPV spectra, Fig. 2(c), the spatial charge evolution can be extracted from the SPV spectra. This time allows discrimination between the time region in which $\langle x\rangle(t)$ increases progressively and that in which $\langle x\rangle(t)$ progressively saturates to a constant value that depends mainly on the sample thickness and slightly on the diffusion coefficient, allowing us to follow qualitatively the spatial charge separation from the SPV transients.

IV. DIFFUSION PHOTOVOLTAGE IN LAYERS THICKER THAN THE SCREENING LENGTH

In this section we will analyze the time evolution of diffusion photovoltage when the layer thickness is larger than the screening length. Let us analyze, as a first approximation to the problem, the important and clarifying case of diffusion without recombination in a semi-infinite space. We consider an initial ($t=0$) sheet of electrons (represented by a delta function) at $x=0$ that diffuses toward positive values of x while the positive charge is fixed at $x=0$. Considering a blocking boundary condition at the origin $x=0$, the solution of the diffusion equation is a semi-Gaussian function,

$$n(x,t)=\frac{n_i}{\sqrt{\pi Dt}}\exp\left(-\frac{x^2}{4Dt}\right), \tag{13}$$

where n_i is the number injected electrons per unit of area.

We have previously[8] calculated the SPV for the electron distribution of Eq. (13) by double integration of the Poisson equation, considering λ_S as the integration limit L_S, where λ_S is related to the Debye-screening length,

$$\text{SPV}(t)=\frac{2en_i}{\sqrt{\pi}\varepsilon\varepsilon_0}\sqrt{Dt}\left(1-\exp\left(-\frac{\lambda_S^2}{4Dt}\right)\right). \tag{14}$$

In general the screening length depends on the local carrier density. In the present experiments λ_S is changing with

time at short times, but it will tend to a constant value at long times. Since in the model of Eq. (14) the screening length only influences the SPV at long times, λ_S is taken as a constant parameter. In the case of a semi-infinite space, Eq. (14) simplifies to

$$\mathrm{SPV}(t) = \frac{2en_i}{\sqrt{\pi}\varepsilon\varepsilon_0}\sqrt{Dt}. \tag{15}$$

The SPV signal increases in time with a slope of 1/2 in a log(SPV) vs log(t) representation. The mean position, i.e., the charge separation length for the given case, is, using Eqs. (8) and (13),

$$\langle x\rangle(t) = \sqrt{\frac{2D\,t}{\pi}}. \tag{16}$$

With this expression and taking into account that $N(t)=n_i$ in the semi-infinite case, the SPV can be also calculated from Eqs. (7) and (16), obtaining the same result as that in Eq. (15).

If we consider the existence of a screening length,[8] the only charge that contributes to the SPV is that placed between $x=0$ and $x=\lambda_S$. Then, $N(t)$ becomes time dependent due to the loss of diffusing charge through the imaginary surface at $x=\lambda_S$. In this case

$$N(t) = n_i\,\mathrm{erf}\left(\frac{\lambda_S}{2\sqrt{D\,t}}\right), \tag{17}$$

where erf(z) is the error function. The mean position with a screening length is, using Eqs. (8), (13), and (17),

$$\langle x\rangle(t) = \sqrt{\frac{4D\,t}{\pi}}\left(1-\exp\left(-\frac{\lambda_S^2}{4Dt}\right)\right)\Bigg/\,\mathrm{erf}\left(\frac{\lambda_S}{2\sqrt{D\,t}}\right). \tag{18}$$

It is easy to find that the SPV can also be calculated from Eqs. (7), (17), and (18), obtaining the same result as that in Eq. (14), as expected from the theoretical discussion of the second section.

Considering the expression (18) as the mean position of the charge, we are now able to follow the spatial charge separation as it is shown in Fig. 3. Figure 3(a) plots the time evolutions of $\langle x\rangle(t)$ for samples with different screening lengths and the same diffusion coefficient. For low times $\langle x\rangle(t)$ evolves with a power law with slope 1/2, as in the case of pure diffusion in a semi-infinite space mentioned above, until for certain t_s, $\langle x\rangle(t)$ reaches a constant value $\langle x\rangle_{ct}=\lambda_S/2$. The appearance of this constant value of the extent of charge separation is due to the finite nature of the region that contributes to the SPV, in contrast with the semi-infinite case studied before. t_s depends on the screening length, and for $t>t_s$ the electron density $\Delta n(x,t)$ is practically uniform in the region between $x=0$ and $x=\lambda_S$ producing the saturation of the $\langle x\rangle(t)$ value to the half of the screening length of the sample.

Figure 3(b) plots the time evolutions of $\langle x\rangle(t)$ for layers of the same thickness with different diffusion coefficients. The value $\langle x\rangle_{ct}=\lambda_S/2$ is obtained for all the samples independently of the diffusion coefficient, indicating that this

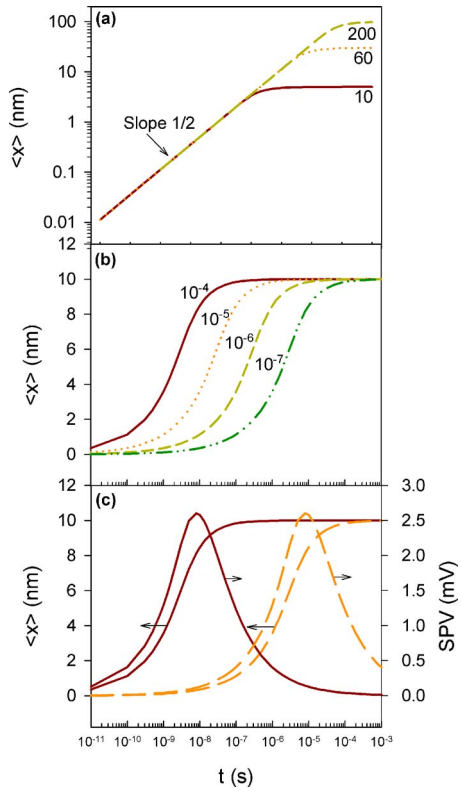

FIG. 3. Calculated mean position $\langle x\rangle(t)$ for the case of normal diffusion considering a screening length, $n_i=10^{11}$ cm^{-2}, $\varepsilon_0=50$. (a) $D=10^{-6}$ cm^2 s^{-1}, for different λ_s, the screening length is indicated, in nm, in the graphic with a number at the same height that $\langle x\rangle_{ct}$ for each curve. (b) $\lambda_s=20$ nm, for different diffusion coefficients, indicated in cm^{-2} s^{-1}. (c) Comparison between the time evolution of SPV, right vertical axis, and $\langle x\rangle(t)$, left vertical axis, considering $\lambda_s=20$ nm and two different diffusion coefficients $D=10^{-4}$ cm^2 s^{-1}, continuous line, and $D=10^{-7}$ cm^2 s^{-1}, dashed line.

magnitude depends only on the screening length, while t_s depends on the diffusion coefficient as well as on the screening length. The spatial charge evolution can be extracted from the SPV spectra as shown in Fig. 3(c). In this case the SPV spectra presents a peak at t_{peak}. During $t<t_{\mathrm{peak}}$, $\langle x\rangle(t)$ evolves as in the case without screening, Eq. (15), following a power law with slope 1/2 in a log(SPV) vs log(t) representation. For $t>t_{\mathrm{peak}}$, $\langle x\rangle(t)$ follows this law progressively until it attains a constant value $\langle x\rangle_{ct}=\lambda_S/2$. This analysis shows that the method that has been introduced constitutes a useful tool to visualize and to study the time evolution of the spatial charge separation.

V. CONCLUSIONS

The analysis of surface photovoltage transients is a powerful method to study the spatial charge separation phenomena in small-scale systems in a wide window of time. The SPV can be split up into two contributions: total amount of charge, and distance between the centers of charge of the positive and negative carrier distributions.

In samples with thickness less than the screening length, the layer thickness has a major role in spatial charge separation, causing the mean position of the charge distribution to reach a constant position $\langle x\rangle_{ct}$ for long times, which depends mainly on the layer thickness and slightly on the diffusion

coefficient. The specific features obtained in the SPV spectra allow following of the time evolution of space-charge separation.

In the case of normal diffusion in a semi-infinite sample $\langle x\rangle(t)$ evolves with a power law with slope 1/2. If a screening length is considered $\langle x\rangle(t)$ evolves with the same power law for low times and attains a constant value $\langle x\rangle_{ct}=\lambda_S/2$ for high times. The transition time between these two regimens can be directly extracted from the t_{peak} of the SPV spectra.

ACKNOWLEDGMENTS

The work was supported by Ministerio de Educación y Ciencia of Spain under Project MAT2004–05168 and Acción Integrada UJI-HMI.

[1]L. Kronik and Y. Shapira, Surf. Sci. Rep. **37**, 1 (1999).
[2]V. Y. Timoshenko, V. Duzhko, and T. Dittrich, Phys. Status Solidi A **182**, 227 (2000).
[3]V. Duzhko, F. Koch, and T. Dittrich, J. Appl. Phys. **91**, 9432 (2002).
[4]V. Duzhko, T. Dittrich, B. Kamenev, V. Y. Timoshenko, and W. Brütting, J. Appl. Phys. **89**, 4410 (2001).
[5]B. Mahrov, G. Boschloo, A. Hagfeldt, L. Dloczik, and T. Dittrich, Appl. Phys. Lett. **84**, 5455 (2004).
[6]T. Dittrich, V. Duzhko, F. Koch, V. Kytin, and J. Rappich, Phys. Rev. B **65**, 155319 (2002).
[7]I. Mora-Seró, T. Dittrich, A. Belaidi, G. Garcia-Belmonte, and J. Bisquert, J. Phys. Chem. B **109**, 14932 (2005).
[8]T. Dittrich, I. Mora-Seró, G. Garcia-Belmonte, and J. Bisquert, Phys. Rev. B **73**, 045407 (2006).
[9]R. H. Young, J. Appl. Phys. **72**, 2993 (1992).
[10]M. M. Perlman, T. J. Sonnonstine, and J. A. S. Pierre, J. Appl. Phys. **47**, 5016 (1976).
[11]G. T. Wright, Solid-State Electron. **2**, 165 (1961).
[12]V. Duzhko, V. Y. Timoshenko, F. Koch, and T. Dittrich, Phys. Rev. B **64**, 075204 (2001).
[13]M. Tachiya and A. Mozuber, Chem. Phys. Lett. **34**, 77 (1975).